Second order adaptive boundary conditions for exterior flow problems: non-symmetric stationary flows in two dimensions

Sebastian Bönisch*

Numerical Analysis group, IWR

University of Heidelberg

sebastian.boenisch@iwr.uni-heidelberg.de

Vincent Heuveline†

Numerical Analysis group, IWR

University of Heidelberg

vincent.heuveline@iwr.uni-heidelberg.de

Peter Wittwer‡

Département de Physique Théorique

Université de Genève, Switzerland

peter.wittwer@physics.unige.ch

Abstract

We consider the problem of solving numerically the stationary incompressible Navier-Stokes equations in an exterior domain in two dimensions. For numerical purposes we truncate the domain to a finite sub-domain, which leads to the problem of finding so called "artificial boundary conditions" to replace the boundary conditions at infinity. To solve this problem we construct – by combining results from dynamical systems theory with matched asymptotic expansion techniques based on the old ideas of Goldstein and Van Dyke – a smooth divergence free vector field depending explicitly on drag and lift and describing the solution to second and dominant third order, asymptotically at large distances from the body. The resulting expression appears to be new, even on a formal level. This improves the method introduced by the authors in a previous paper and generalizes it to non-symmetric flows. The numerical scheme determines the boundary conditions and the forces on the body in a self-consistent way as an integral part of the solution process. When compared with our previous paper where first order asymptotic expressions were used on the boundary, the inclusion of second and third order asymptotic terms further reduces the computational cost for determining lift and drag to a given precision by typically another order of magnitude.

Mathematics Subject Classification (2000). 76D05, 76D25, 76M10, 41A60, 35Q35.

Keywords. Navier-Stokes equations, artificial boundary conditions, drag, lift.

1 Introduction

Exterior flows at low Reynolds numbers – of the order of one to several thousand – play an increasingly important role in applications. Specific examples of situations where such flows occur are the sedimentation of small particles in the context of climate prediction [2], [42] and the engineering of wings in the design of miniature aircraft [32], [9]. In all cases the forces exerted on the body need do be computed accurately.

In the present work we limit ourselves to the case of two-dimensional stationary incompressible flows. Linearized theories (Stokes, Oseen) provide a quantitative description of such situations for Reynolds numbers less than one [4], and traditional approximation schemes based of some version of boundary layer theory [36], [11], [12] provide a quantitative description for the case of Reynolds numbers larger

than some ten thousand. For the intermediate regime, where neither the viscous forces nor the inertial forces dominate, the full Navier-Stokes equations need to be solved.

So, consider a rigid body that is placed into a uniform stream of a homogeneous incompressible fluid filling up all of $\mathbf{R}^2$. This situation is modeled by the stationary Navier-Stokes equations

$$-\rho\left(\tilde{\mathbf{u}}\cdot\nabla\right)\tilde{\mathbf{u}}+\mu\Delta\tilde{\mathbf{u}}-\nabla\tilde{p}=0\ , \tag{1}$$

$$\nabla\cdot\tilde{\mathbf{u}}=0\ , \tag{2}$$

in $\tilde{\Omega}=\mathbf{R}^2\setminus\tilde{\mathbf{B}}$, with $\tilde{\mathbf{B}}$ a compact set (the body) containing the origin of our coordinate system, subject to the boundary conditions

$$\tilde{\mathbf{u}}|_{\partial\tilde{\mathbf{B}}}=0\ , \tag{3}$$

$$\lim_{|\tilde{\mathbf{x}}|\to\infty}\tilde{\mathbf{u}}(\tilde{\mathbf{x}})=\tilde{\mathbf{u}}_\infty\ . \tag{4}$$

Here, $\tilde{\mathbf{u}}$ is the velocity field, $\tilde{p}$ is the pressure and $\tilde{\mathbf{u}}_\infty$ is some constant non-zero vector field which we choose without restriction of generality to be parallel to the $\tilde{x}$-axis, $i.e.$, $\tilde{\mathbf{u}}_\infty=u_\infty\mathbf{e}_1$, where $\mathbf{e}_1=(1,0)$ and $u_\infty>0$. The density ρ and the viscosity μ are arbitrary positive constants. From μ, ρ and u_∞ we can form the length ℓ,

$$\ell=\frac{\mu}{\rho u_\infty}\ , \tag{5}$$

the so called viscous length of the problem. The viscous forces and the inertial forces are quantities of comparable size if the diameter A of $\tilde{\mathbf{B}}$ is comparable with ℓ, $i.e.$, if the Reynolds number

$$\mathrm{Re}=\frac{A}{\ell}\ , \tag{6}$$

is neither very small nor very large. Below, we will study flows with Reynolds numbers in the range from one to several thousand. Note that for bodies with smooth boundary $\partial\tilde{\mathbf{B}}$ and for small enough Reynolds numbers (6) equation (1), (2) subject to the boundary conditions (3), (4) is known to have a strong solution [13], [14]. For large Reynolds numbers this is still an open problem [17].

When solving the problem (1)-(4) numerically by restricting the equations from the exterior infinite domain $\tilde{\Omega}$ to (a sequence of) bounded domains $\tilde{\mathbf{D}}\subset\tilde{\Omega}$ (see Figure 2), one is confronted with the necessity of finding appropriate boundary conditions on the surface $\tilde{\Gamma}=\partial\tilde{\mathbf{D}}\setminus\partial\tilde{\mathbf{B}}$ of the truncated domain. In a recent paper [6] we have introduced a novel self-consistent scheme that uses on the boundary the vector field obtained from an asymptotic analysis of (1), (2) and (4) to leading order [47], [49], [23]. Here, by using matched expansion techniques, we construct a smooth divergence free vector field that satisfies the boundary condition (4) and solves the stationary Navier-Stokes equations (1) to second and dominant third order, asymptotically at large distances from the body. This vector field is given in the form of an explicit expression depending on two real parameters which can be determined from the drag and the lift exerted on the body. Using this vector field to prescribe artificial boundary conditions on $\tilde{\Gamma}$ we set up a self-consistent scheme that determines the two parameters and hence the boundary conditions and the forces on the body as an integral part of the solution process. For related ideas concerning artificial boundary conditions see [33], [3], [24].

For the construction of the asymptotic expansion used here we follow closely the old ideas of Goldstein [22] and Van Dyke [40], supplemented with the more recent ideas from dynamical systems theory [18]. It is these improvements that allow us to use the results as artificial boundary conditions for numerical purposes, or as the starting point for rigorous mathematical work [23], [48]. In particular, we properly address questions related with the boundary condition (4) and the regularity of the resulting vector fields across the $\tilde{x}$-axis within the wake. All the formal work has been done using the computer-algebra system Maple.

The method presented here improves the scheme introduced in our previous paper [6] and generalizes it to the situation of non-symmetric stationary flows. In [6], the computation times necessary to determine the drag with a given precision were typically several orders of magnitude reduced when compared to using homogeneous Dirichlet boundary conditions. The inclusion of higher order asymptotic terms on the boundary reduces computational times further, typically by yet another order of magnitude. Figure 1 is an example of what can be computed with our setup. It shows the flow around the NACA profile 64-915, inclined by $5°$, at Reynolds number (6) one thousand, with A the chord length of the profile (distance

2

from tip to tail) [30]. Our results quite nicely illustrate the scientific potential of a combined use of modern techniques from analysis and geometry, formal algebraic computation systems and numerical simulations.
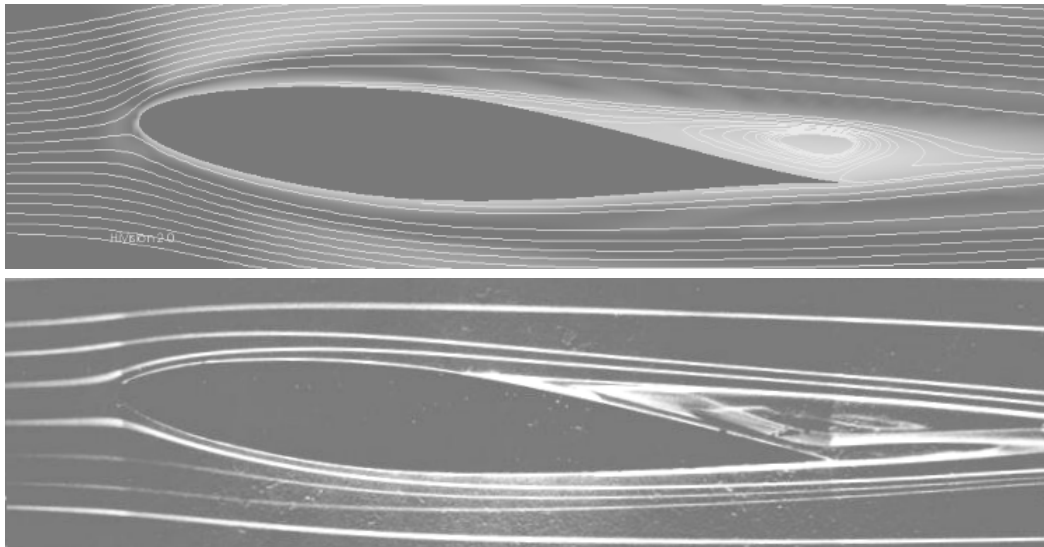

Figure 1. Flow around the NACA profile 64-015 at Reynolds number one thousand as computed with second order adaptive boundary conditions (top) and experimental flow around the NACA profile 64A015 (bottom). Bottom image: courtesy of ONERA (H. Werlé, 1974, [44]).

2 Artificial boundary conditions

In this section we derive the boundary conditions used in later sections. The discussion will be formal. For the wake region the correctness of the resulting expressions is up to first order proved in [23]. A complete mathematical proof of the second and third order asymptotics presented here is in preparation and will be published elsewhere.

There exists an extensive literature on matched asymptotic expansions for laminar flows [5], [10], [40], [31], [37]. Most of the work is however either limited to symmetric flows or uses as a starting point not the Navier-Stokes equations but some version of boundary layer theory. As an example, for the symmetric case, results for the so-called centerline velocity (the velocity on the symmetry axis of the body in the wake region) up to third order is given in [38], [37]. Our results show that the expansions computed from the Navier-Stokes equations differ from the ones computed from boundary layer theory already to second order, so that higher order results based on boundary layer theory are inadequate for modeling Navier-Stokes flows. An other problem of existing work is that the boundary conditions and the regularity of the solution are only imposed asymptotically, rather than term by term. For some applications such an approach may be sufficient, but it is obviously insufficient for the use of such expansions as artificial boundary conditions. As a result the expressions derived here appear to be new, even on a formal level.

Before proceeding any further we now rewrite the Navier-Stokes equations in dimensionless form. Let $\tilde{\mathbf{u}}$ be the velocity field and $\tilde{p}$ the pressure introduced in (1)-(4), and let ℓ be as defined in (5). Then, we define dimensionless coordinates $\mathbf{x} = \tilde{\mathbf{x}}/\ell$, and introduce a dimensionless vector fields $\mathbf{u}$ and a dimensionless pressure p through the definitions

$$\tilde{\mathbf{u}}(\tilde{\mathbf{x}}) = u_\infty \mathbf{u}(\mathbf{x}) \; , \tag{7}$$

$$\tilde{p}(\tilde{\mathbf{x}}) = (\rho u_\infty^2) p(\mathbf{x}) \; . \tag{8}$$

In the new coordinates we get instead of (1)-(4) the equations

$$-\left(\mathbf{u} \cdot \nabla\right) \mathbf{u} + \Delta \mathbf{u} - \nabla p = 0 \; , \tag{9}$$

$$\nabla \cdot \mathbf{u} = 0 \; , \tag{10}$$

in $\Omega = \mathbf{R}^2 \setminus \mathbf{B}$, where

$$\mathbf{B} = \left\{ \mathbf{x} \in \mathbf{R}^2 \,|\, \ell \mathbf{x} = \tilde{\mathbf{x}} \text{ for some } \tilde{\mathbf{x}} \in \tilde{\mathbf{B}} \right\} \,,$$

and the boundary conditions

$$\mathbf{u}|_{\partial \mathbf{B}} = 0 \,, \tag{11}$$

$$\lim_{|\mathbf{x}| \to \infty} \mathbf{u}(\mathbf{x}) = (1,0) \,. \tag{12}$$

In (9)-(10) all derivatives are with respect to the new coordinates.

2.1 The vorticity equation

Let $\mathbf{u} = (u,v)$, and let

$$\omega(x,y) = -\partial_y u(x,y) + \partial_x v(x,y) \,. \tag{13}$$

The function ω is the vorticity of the fluid. By taking the curl of (9) we get the equation

$$W(u,v,\omega) \equiv -(\mathbf{u} \cdot \nabla)\omega + \Delta\omega = 0 \,. \tag{14}$$

Once (10) and (14) are solved for $\mathbf{u}$ and ω, the pressure p can be constructed by solving the equation that we get by taking the divergence of (9) subject to the appropriate boundary conditions.

There is plenty of experimental, numerical and theoretical evidence that the vorticity ω decays very rapidly (faster than exponential) away from the body except within the wake region [1]. Recent mathematical results [43], [19], [20], [23] suggest the existence of functions ω_n with support in $\Omega_+ = \{(x,y) \in \Omega \,|\, x > 0\}$ such that

$$\omega(x,y) \approx \sum_{n \geq 1} \omega_n(x,y) \,, \tag{15}$$

asymptotically as $x \to +\infty$, in the sense that for all $N \geq 1$

$$\lim_{x \to \infty} x^{\frac{1+N}{2}} \sup_{y \in \mathbf{R}} \left| \omega(x,y) - \sum_{n=1}^{N} \omega_n(x,y) \right| = 0 \,. \tag{16}$$

More precisely, the functions ω_n are conjectured to be of the form

$$\omega_n(x,y) = \sum_{m=1}^{n} \rho_{n,m}(x)\varphi_{n,m}''(\frac{y}{\sqrt{x}}) \,, \tag{17}$$

for certain smooth functions $\varphi_{n,m}$ with derivatives $\varphi_{n,m}'$, $\varphi_{n,m}''$ decaying at infinity faster than exponential and

$$\rho_{n,m}(x) = \frac{\log(x)^{n-m}}{x^{(1+n)/2}} \,. \tag{18}$$

The main ideas of a proof of (16) for $N = 1$ and small enough Reynolds numbers can be found in [23] and a complete mathematical proof of (15)-(18) up to $N = 3$ is in preparation. For $N > 3$ (15)-(18) are purely conjectural.

Here, we stay on a formal level and explain the construction of the functions $\varphi_{n,m}$ for $1 \leq m \leq 2$ and $1 \leq n \leq 3$ by asymptotic expansion techniques, using (14) as a starting point. These formal results are then used for the purpose of prescribing artificial boundary conditions. As a consequence the numerical experiments of Section 4 not only show the usefulness of asymptotic expressions for simulation purposes, but at the same time provide interesting quantitative information concerning the convergence of the limits in (16).

The main problem with (14) is that it involves in addition to the vorticity ω also the velocity $\mathbf{u}$. For this reason, the traditional approach for constructing an asymptotic expansions is to use an ad hoc ansatz for the stream function ψ from which one then computes expansions for u and v and ω via

$$u(x,y) = \partial_y \psi(x,y) \,, \tag{19}$$

$$v(x,y) = -\partial_x \psi(x,y) \,, \tag{20}$$

4

and

$$\omega(x, y) = -\Delta\psi(x, y) \ , \tag{21}$$

which are then plugged into (14) and solved order by order. The stream function has however a more complicated structure than the vorticity and in spite of the efforts of various authors the matched asymptotic expansion for ψ of the traditional ansatz is plagued with all sorts of inconsistencies concerning the boundary condition (4) and the regularity of the resulting terms across the x-axis in the wake region. Here we solve this problem by avoiding this ad hoc ansatz. The basic observation is that from the vorticity ω and its downstream asymptotic expansion (15) an expansion of the stream function can be obtained simply by using the definitions (see next paragraph). The terms of the old ad hoc ansatz can then be recovered together with certain new terms that solve the problems concerning the boundary conditions and the regularity.

So, let ω be given. Then, the stream function ψ has to satisfy (21) in Ω, subject to the boundary conditions

$$\psi|_{\partial\mathbf{B}} = 0 \ , \tag{22}$$

$$\partial_{\mathbf{n}}\psi|_{\partial\mathbf{B}} = 0 \ , \tag{23}$$

$$\lim_{x,y\to\infty} -\partial_x\psi(x, y) = 0 \ , \tag{24}$$

$$\lim_{x,y\to\infty} \partial_y\psi(x, y) = 1 \ . \tag{25}$$

Equations (22) and (23) are equivalent to (11), and (24) and (25) are equivalent to (12). Note that the system of equations (21)-(25) is a priori over-determined since for a general problem of the form (21) only (22) (Dirichlet problem) or (23) (Neumann problem) can be imposed. The fact that the Navier-Stokes problem (1)-(4) is well posed has the important implication that the vorticity ω is such that (22) and (23) are equivalent, *i.e.*, lead to the same solution ψ. In any case, let

$$\psi_\omega = -G * \omega \ , \tag{26}$$

with $*$ the convolution product and

$$G(x, y) = \frac{1}{2\pi} \operatorname{Re}\left[\log(-x - iy)\right] = \frac{1}{4\pi} \log(x^2 + y^2) \ .$$

From (22)-(25) it then follows using general results from potential theory that

$$\psi(x, y) = y + \psi_\omega(x, y) + h(x, y) \ , \tag{27}$$

with h a harmonic function in Ω, satisfying the bound

$$|h(x, y)| \le \frac{\text{const.}}{r} \ , \tag{28}$$

where $r = \sqrt{x^2 + y^2}$. The partial derivatives of h with respect to x and y obey analogous bounds. Note that the function h depends explicitly on the boundary conditions on $\partial\mathbf{B}$ and can therefore not be determined from large distance asymptotic expansions alone. For the function ψ_ω we will use below for $N \ge 1$ the decomposition

$$\psi_\omega = \psi_N + R_N \ , \tag{29}$$

where

$$\psi_N = 2b_N \, G - \sum_{n=1}^{N} G * \omega_n \ , \tag{30}$$

with

$$b_N = b + \frac{1}{2} \sum_{n=1}^{N} \int_\Omega \omega_n(x, y) \, dxdy \ ,$$

and with

$$b = -\frac{1}{2} \int_\Omega \omega(x, y) \, dxdy \ , \tag{31}$$

5

and we will show formally that for $N > 3$

$$|R_N(x,y)| \leq \frac{\text{const.}}{r} \ , \tag{32}$$

and similar for partial derivatives. On a heuristic level it follows from the bounds (28) and (32) that one should not hope to be able to determine approximations to ψ from large distance asymptotics alone for $N > 3$, and there appears indeed to be no straightforward way to extend the asymptotic scheme presented here to yet higher order (see [20] for limitations of the same type in a related case).

Basically, the idea is now to use the functions ψ_N as an approximation to ψ in order to compute approximations u_N and v_N for u and v using (19) and (20). These approximations are then plugged together with (15) into (14) in order to obtain equations for the functions ω_n. This way, by construction, the functions u_N and v_N are smooth in Ω and decay at infinity as required by (4). This solves the above mentioned consistency problems of the ad hoc procedures found in the literature at the price of introducing non-local expressions for u_N and v_N do to the convolution products in (30). Such non-local expressions are neither manipulated easily when trying to solve the resulting equations for ω_n, nor used easily for the prescription of boundary conditions for numerical purposes. For $N \leq 3$ we have therefore analyzed these convolution products in detail, and it turns out that, modulo terms bounded again by const./r, local approximations to these convolution products can be constructed. The resulting expressions are indeed similar to those used in the ad hoc procedures of earlier work, but additional terms arise which restore the regularity of the local approximations. Explicitly, we find the following functions for the first couple of terms in (15), (17) (see Appendix I),

$$\varphi_{1,1}(z) = d \ \text{erf}(\frac{z}{2}) \ ,$$

$$\varphi_{2,1}(z) = bd \ \frac{1}{\pi^{3/2}} e^{-\frac{z^2}{4}} \ ,$$

$$\varphi_{2,2}(z) = -d^2 \ f(z) + b \ c_{2,2} \ e^{-\frac{z^2}{4}} \ ,$$

$$\varphi_{3,1}(z) = -b^2 d \ \frac{z}{4\pi^{5/2}} e^{-\frac{z^2}{4}} \ . \tag{33}$$

Here erf is the error function, $i.e.$, $\text{erf}(z) = \frac{2}{\sqrt{\pi}} \int_0^z \exp(-\zeta^2) d\zeta$, and $f \colon \mathbf{R} \to \mathbf{R}$ is the unique solution of the third order linear in-homogeneous ordinary differential equation

$$f'''(z) + \frac{1}{2} z f''(z) + f'(z) + \frac{1}{2\pi} e^{-\frac{1}{2}z^2} = 0 \ , \tag{34}$$

satisfying $f(0) = 0$, $f'(0) = -\frac{1}{2\pi}$, $f''(0) = 0$. Note that f is an odd function and that f' and f'' decay faster than exponential at infinity. Moreover

$$f_\infty = \lim_{z \to \infty} f(z) = -\frac{1}{\sqrt{2\pi}} \ . \tag{35}$$

See Figure 3 for a graph of the function f. For the constant b as defined in (31) and for the constant d we have (see Appendix II),

$$d = \frac{1}{2} \frac{1}{\rho \ell u_\infty^2} \tilde{F} \ ,$$

$$b = \frac{1}{2} \frac{1}{\rho \ell u_\infty^2} \tilde{L} \ , \tag{36}$$

with $\tilde{F}$ the drag and $\tilde{L}$ the lift acting on the body (dimension-full quantities), and ℓ as defined in (5). The constant $c_{2,2}$ can not be determined from drag and lift alone, $i.e.$, the expansion of the even part of the vorticity (with respect to y) can be computed as indicated up to the term $\varphi_{2,1}$ only. The odd part of the vorticity can be computed up to the term $\varphi_{3,1}$. For more details see the Appendix I. In most of what follows we set $c_{2,2}$ as well as the functions $\varphi_{3,2}$ and $\varphi_{3,3}$ and all higher order terms equal to zero.

2.2 Asymptotic expansion for u and p

In Appendix I we compute together with (33) the following local approximations to $\mathbf{u} = (u, v)$:

$$\mathbf{u}_N(x, y) = \mathbf{e}_1 + \sum_{n=1}^{N} \sum_{m=1}^{n} \mathbf{u}_{n,m}(x, y) ,$$

where $\mathbf{e}_1 = (1, 0)$. To first order we have

$$u_{1,1}(x, y) = u_{1,1,E}(x, y) - \theta(x) \frac{d}{\sqrt{\pi}} \frac{1}{\sqrt{x}} e^{-\frac{y^2}{4x}} ,$$

$$v_{1,1}(x, y) = v_{1,1,E}(x, y) - \theta(x) \frac{d}{2\sqrt{\pi}} \frac{y}{x^{3/2}} e^{-\frac{y^2}{4x}} , \tag{37}$$

with θ the Heaviside function (i.e., $\theta(x) = 1$ for $x > 0$ and $\theta(x) = 0$ for $x < 0$), and

$$u_{1,1,E}(x, y) = \frac{d}{\pi} \frac{x}{x^2 + y^2} + \frac{b}{\pi} \frac{y}{x^2 + y^2} ,$$

$$v_{1,1,E}(x, y) = \frac{d}{\pi} \frac{y}{x^2 + y^2} - \frac{b}{\pi} \frac{x}{x^2 + y^2} . \tag{38}$$

Note that the vector field $(u_{1,1}, v_{1,1})$ in (37) is divergence free and smooth in $\mathbf{R}^2 \setminus \{0\}$. For $b = 0$ this is the vector field that has been used for prescribing artificial boundary conditions in our previous paper [6]. The additional term with amplitude b is the vector field of a point vortex and is responsible for a nonzero lift (see Appendix II, and see [23] for a proof that this is the dominant asymmetric term far downstream). To second order we find

$$u_{2,1}(x, y) = \theta(x) \frac{bd}{2} \frac{1}{(\sqrt{\pi})^3} \frac{\log(x)}{x} \frac{y}{\sqrt{x}} e^{-\frac{y^2}{4x}} ,$$

$$v_{2,1}(x, y) = \theta(x) \frac{bd}{2} \frac{1}{(\sqrt{\pi})^3} \frac{1}{x^{3/2}} \left(\log(x) \left(-1 + \frac{1}{2} \frac{y^2}{x} \right) + 2 \right) e^{-\frac{y^2}{4x}} , \tag{39}$$

and

$$u_{2,2}(x, y) = u_{2,2,E}(x, y) + \theta(x) d^2 \frac{1}{x} f'(\frac{y}{\sqrt{x}})$$
$$+ \lambda \theta(x) f_\infty d^2 \frac{3}{8} \frac{1}{x^2} \left((1 + \frac{|y|}{\sqrt{x}})(1 - \frac{1}{2} \frac{y^2}{x}) + \frac{|y|}{\sqrt{x}} \right) e^{-\frac{y^2}{4x}} ,$$

$$v_{2,2}(x, y) = v_{2,2,E}(x, y) + \theta(x) \frac{d^2}{2} \frac{1}{x^{3/2}} \left(\left(f(\frac{y}{\sqrt{x}}) - f_\infty \text{sign}(y) \right) + \frac{y}{\sqrt{x}} f'(\frac{y}{\sqrt{x}}) \right)$$
$$+ \lambda \theta(x) f_\infty d^2 \frac{3}{4} \frac{1}{x^{5/2}} \left((1 + \frac{|y|}{\sqrt{x}}) \frac{y}{\sqrt{x}} \left(1 - \frac{1}{8} \frac{y^2}{x} \right) + \frac{1}{4} \frac{y^2}{x} \text{sign}(y) \right) e^{-\frac{y^2}{4x}} , \tag{40}$$

where

$$u_{2,2,E}(x, y) = f_\infty \frac{d^2}{2} \frac{|y|}{r^2} \left(\frac{1}{r_2} - \frac{r_2}{r} \right) ,$$

$$v_{2,2,E}(x, y) = f_\infty \frac{d^2}{2} \frac{\text{sign}(y)}{r} \left(-\frac{1}{r_2} - \frac{x}{r_2 r} + \frac{x \, r_2}{r^2} \right) , \tag{41}$$

with $r = \sqrt{x^2 + y^2}$, $r_2 = \sqrt{2r + 2x}$, $\lambda = 1$, and f_∞ as defined in (35). Note that the terms proportional to λ are higher order and one might be tempted to neglect them, i.e., to set $\lambda = 0$. This is not possible, however, without giving up the regularity of the second order derivatives $\partial_y^2 u$ and $\partial_y^2 v$ across the positive x-axis (see Appendix I). Finally, to third order we find

$$u_{3,1}(x, y) = \theta(x) \frac{b^2 d}{4} \frac{1}{(\sqrt{\pi})^5} \frac{\log(x)^2}{x^{3/2}} \left(1 - \frac{1}{2} \frac{y^2}{x} \right) e^{-\frac{y^2}{4x}} ,$$

$$v_{3,1}(x, y) = \theta(x) \frac{b^2 d}{2} \frac{1}{(\sqrt{\pi})^5} \frac{\log(x)}{x^2} \frac{y}{\sqrt{x}} \left(\frac{\log(x)}{4} \left(3 - \frac{1}{2} \frac{y^2}{x} \right) - 1 \right) e^{-\frac{y^2}{4x}} , \tag{42}$$

7

and we set all the other third order terms equal to zero (they can not be computed from drag and lift alone). We finally note that once the approximate expressions for the velocity field $\mathbf{u}$ are known, similar approximations can be computed for the pressure. For the computation of drag and lift (see Appendix II) we only need the first order approximation, *i.e.*, $p \approx p_1$, where

$$p_1(x, y) = -\frac{1}{2} \left((1 + u_{1,1,E}(x, y))^2 - 1 + v_{1,1,E}^2(x, y) \right) , \tag{43}$$

with the normalization $\lim_{x,y \to \infty} p_1(x, y) = p(x, y) = 0$.

2.3 Adaptive boundary conditions of order N

In order to solve (1) numerically, it is more convenient to set $\tilde{\mathbf{u}} = \tilde{\mathbf{u}}_\infty + \tilde{\mathbf{v}}$, and to study the equation

$$-\rho \left(\tilde{\mathbf{u}}_\infty \cdot \nabla \right) \tilde{\mathbf{v}} - \rho \left(\tilde{\mathbf{v}} \cdot \nabla \right) \tilde{\mathbf{v}} + \mu \Delta \tilde{\mathbf{v}} - \nabla \tilde{p} = 0 ,$$
$$\nabla \cdot \tilde{\mathbf{v}} = 0 , \tag{44}$$

subject to the boundary conditions

$$\tilde{\mathbf{v}}|_{\partial \tilde{\mathbf{B}}} = -\tilde{\mathbf{u}}_\infty , \tag{45}$$
$$\lim_{|\tilde{\mathbf{x}}| \to \infty} \tilde{\mathbf{v}}(\tilde{\mathbf{x}}) = 0 . \tag{46}$$

The equations (44) are then discretized in a truncated domain $\tilde{\mathbf{D}}$, and the boundary condition (46) is replaced by the boundary conditions

$$\tilde{\mathbf{v}}|_{\tilde{\Gamma}} = \tilde{\mathbf{v}}_{ABC} , \tag{47}$$

with $\tilde{\mathbf{v}}_{ABC}(\tilde{x}, \tilde{y}) = u_\infty \, \mathbf{v}_N(x, y)$, where $\mathbf{v}_N(x, y) = \sum_{n=1}^{N} \sum_{m=1}^{n} \mathbf{u}_{n,m}(x, y)$, $x = \tilde{x}/\ell$, $y = \tilde{y}/\ell$ with ℓ as defined in (5), and where $N = 0$ (homogeneous Dirichlet data), $N = 1$ (first order adaptive boundary conditions; see [6] and below), or $N = 2$ or 3 (second, respectively third order adaptive boundary conditions; see below).

3 Solution process

In what follows we give details concerning the discretization procedure and the algorithms that we use to solve (44), (45), (47) numerically. To unburden the notation we suppress throughout this section the "tildes".

3.1 Galerkin finite element discretization

In order to solve equation (44), we consider a discretization based on conforming mixed finite elements with continuous pressure. This discretization starts from a variational formulation of the system of equations (44). First, we introduce some notation needed for the derivation of this formulation.

For a bounded domain $\mathbf{D} \subset \mathbf{R}^2$, let $L^2(\mathbf{D})$ denote the Lebesgue space of square-integrable functions on $\mathbf{D}$ equipped with the inner product and norm

$$(f, g)_{\mathbf{D}} = \int_{\mathbf{D}} fg \, d\mathbf{x} , \qquad ||f||_{\mathbf{D}} = (f, f)_{\mathbf{D}}^{1/2} .$$

The pressure is assumed to lie in the space $L_0^2(\mathbf{D}) := \{q \in L^2(\mathbf{D}) \,|\, \int_{\mathbf{D}} q \, d\mathbf{x} = 0\}$, which defines it uniquely. The $L^2(\mathbf{D})$ functions with generalized (in the sense of distributions) first-order derivatives in $L^2(\mathbf{D})$ form the Sobolev space $H^1(\mathbf{D})$, while $H_0^1(\mathbf{D}) := \{v \in H^1(\mathbf{D}) \,|\, v|_{\partial \mathbf{D}} = 0\}$. Let $W = [H_0^1(\mathbf{D})]^2 \times L_0^2(\mathbf{D})$. For $\mathbf{w} = \{\mathbf{v}, p\} \in W$ and $\phi = \{\varphi, q\} \in W$, we define the semi-linear form

$$\mathcal{A}(\mathbf{w}; \phi) = \rho \left(((\mathbf{v} + \mathbf{u}_\infty) \cdot \nabla)\mathbf{v}, \varphi \right)_{\mathbf{D}} - (p, \nabla \cdot \varphi)_{\mathbf{D}} + 2\mu \int_{\mathbf{D}} \mathcal{D}(\mathbf{v}) : \mathcal{D}(\varphi) \, d\mathbf{x} - (\nabla \cdot \mathbf{v}, q)_{\mathbf{D}} , \tag{48}$$

which is obtained by testing the equations (44) with $\phi \in W$ and by integration by parts of the diffusive term and the pressure gradient (see *e.g.* [34, 15, 16, 39, 27] for more details). $\mathcal{D}(\mathbf{v})$ denotes the deformation

tensor, i.e., $\mathcal{D}(\mathbf{v}) = \frac{1}{2}(\nabla \mathbf{v} + (\nabla \mathbf{v})^T)$. Then, a weak form of the equations (44) can be formulated as: find $\mathbf{w} = \{\mathbf{v}, p\} \in W$, such that

$$\mathcal{A}(\mathbf{w}; \phi) = 0 , \quad \forall \phi \in W . \tag{49}$$

The discretization of problem (49) uses a conforming finite element space $W_h \subset W$ defined on quasi-uniform triangulations $\mathcal{T}_h = \{K\}$ consisting of quadrilateral cells K covering the domain $\mathbf{D}$. We consider the standard Hood-Taylor finite elements [28] for the trial and test spaces, i.e., we define

$$W_h = \left\{ (\mathbf{v}, p) \in [C(\overline{\mathbf{D}})]^3 \mid \mathbf{v}|_K \in [Q_2]^2, \ p|_K \in Q_1 \right\} ,$$

where Q_r describes the space of isoparametric tensor-product polynomials of degree r (for a detailed description of this standard construction process see for example [7]). This choice for the trial and test functions guarantees a stable approximation of the pressure since the Babuska-Brezzi inf-sup stability condition is satisfied uniformly in $\mathbf{D}$ (see [8] and references therein). The advantage, when compared to equal order function spaces for the pressure and the velocity, is that no additional stabilization terms are needed. The discrete counterpart of problem (49) then reads: find $\mathbf{w}_h = \{\mathbf{v}_h, p_h\} \in \mathbf{w}_{b,h} + W_h$, such that

$$\mathcal{A}(\mathbf{w}_h; \phi_h) = 0 , \quad \forall \phi_h \in W_h . \tag{50}$$

Here $\mathbf{w}_{b,h}$ describes the prescribed Dirichlet data on the boundary $\mathbf{\Gamma}$ of the domain $\mathbf{D}$. A straightforward approach consists in considering a domain $\mathbf{D}$ which is large enough such that $\mathbf{v}$ is vanishingly small in $\Omega \backslash \mathbf{D}$. As shown in [6] this approach, which corresponds to imposing homogeneous Dirichlet boundary conditions for $\mathbf{v}$ on Γ, generally leads to extremely large and intractable discrete problems. Our goal is to avoid these difficulties by imposing adequate non-homogeneous Dirichlet boundary conditions on $\mathbf{\Gamma}$. As explained in Section 2, the proposed artificial boundary conditions are independent of the details of the geometry of the body but depend explicitly on drag and lift. The accurate determination of these forces is therefore a key issue in our context. As in [6] we use the approach proposed in [21] which is based on a reformulation of the expressions for drag and lift in terms of volume integrals by means of integration by parts. This reformulation allows to attain the full order of convergence for the values of drag and lift.

3.2 The solver

The nonlinear algebraic system (50) is solved implicitly in a fully coupled manner by means of a damped Newton method. Denoting the derivative of $\mathcal{A}(\cdot, \cdot)$ taken at a discrete function $\mathbf{w}_h \in W_h$ by $\mathcal{A}'(\mathbf{w}_h, \cdot)(\cdot)$, the linear system arising at the Newton step number k has the following form,

$$\mathcal{A}'(\mathbf{w}_h^k, \phi_h)(\hat{\mathbf{w}}_h^k) = (\mathbf{r}_h^k, \phi_h) , \quad \forall \phi_h \in W_h , \tag{51}$$

where $\mathbf{r}_h^k$ is the equation residual of the current approximation $\mathbf{w}_h^k$, and where $\hat{\mathbf{w}}_h^k$ corresponds to the needed correction. The updates $\mathbf{w}_h^{k+1} = \mathbf{w}_h^k + \alpha^k \hat{\mathbf{w}}_h^k$ with a relaxation parameter α^k chosen by means of Armijo's rule are carried out until convergence. In practice, the Jacobian involved in (51) is directly derived from the analytical expression for the derivative of the variational system (50).

It is well known that the ability of the Newton iteration to converge at the local rate greatly depends on the quality of the initial approximation (see e.g. [29]). In order to find such an initial approximation, we consider a mesh hierarchy $\mathcal{T}_{h_l}$ with $\mathcal{T}_{h_l} \subset \mathcal{T}_{h_{l+1}}$, and the corresponding system of equations (50) is successively solved by taking advantage of the previously computed solution, i.e., the nonlinear Newton steps are embedded in a nested iteration process (see e.g. [45], chapter 8).

The linear subproblems (51) are solved by the *Generalized Minimal Residual Method* (GMRES), see Saad [35], preconditioned by means of multigrid iterations. See [46, 45] and references therein for a description of the different multigrid techniques for flow simulations. This preconditioner, based on a new multigrid scheme oriented towards conformal higher order finite element methods, is a key ingredient of the overall solution process. Two specific features characterizing the proposed scheme are: varying order of the finite element ansatz on the mesh hierarchy and a Vanka type smoother [41] adapted to higher order discretization. This somewhat technical part of the solver is described in full details in [26]. Its implementation is part of the HiFlow project (see [25]).

To summarize, the specificity of our approach is to prescribe boundary conditions which depend on the drag and the lift. These values, and therefore the adequate boundary conditions, are not known at the beginning of the resolution process. Therefore, the Newton steps previously described are embedded in an additional fixed point iteration which determines the boundary conditions through successive updates, based on the previously computed values of drag and lift.

4 Numerical experiments

The proposed adaptive boundary conditions (37-42) have a complicated structure. Our goal in this section is to quantify the impact of the various terms of these boundary conditions on the accuracy of the solution. For that purpose we will consider the five variants of boundary conditions as depicted in Table 1, ranging from the pure first order boundary conditions to the full second order boundary conditions that include the nonzero lift effects. See (36) for the expressions relating b to the lift and d to the drag. Throughout this section we suppress the "tildes" from the notation and we write (u, v) for the components of the (numerical) solution $\mathbf{v}$ of (44).

First, we discuss the case of a symmetric body which consists of a rectangle $[-0.1, 0.1] \times [-0.5, 0.5]$ immersed into a uniform stream of a homogeneous incompressible fluid with density $\rho = 1$ and dynamic viscosity $\mu = 0.1$. We impose furthermore $u_\infty = 0.1$. With $A = 1$ being the length of the rectangle, we find from (5) that $\ell = 1$ and therefore with (6) the Reynolds number Re = 1. This configuration has already been investigated using first order boundary conditions in [6]. On the basis of this benchmark configuration our goal is to examine the gain obtained by means of the additional second order terms. Note that due to the symmetry of the body the lift and therefore b is equal to zero. Therefore, the variants denoted by (sym/sym), (nonsym/sym) and (nonsym/nonsym) in Table 1 are all equivalent. A quantity of importance in this context is the so called centerline velocity $u(x, 0)$. It has been extensively studied (see for example [38] and [37]), as its behavior for (large) positive x reveals information on the asymptotics of the wake. From (37) we get using (7) the theoretical prediction that in dimension-full variables to leading order for large x,

$$u(x, 0) \approx \left(u_\infty \sqrt{\ell} \right) \frac{c}{2\sqrt{\pi}} \frac{1}{\sqrt{x}} , \tag{52}$$

with $c = -2d$ and d as defined in (36), *i.e.*, $c = -\tilde{F}/(\rho \ell u_\infty^2)$. Numerically we find that $\tilde{F} = 0.05029$. In Figure 4 we have plotted the quantity $-2\sqrt{\pi}\sqrt{x}u(x, 0)$ as a function of x, where u has been computed once using first order boundary conditions and once using the second order adaptive boundary conditions. With second order boundary conditions the plot is closer to the asymptotic value on most of the domain. The impact of the second order terms is however much more evident when considering the gain with regard to the relative error of the drag. In the plots of Figure 5, the relative error of the drag as a function of the domain diameter is plotted considering the homogeneous Dirichlet boundary conditions, the first order boundary conditions (sym) and the second order boundary conditions (sym/sym). Clearly, the addition of the second order terms allow to again substantially reduce the size of the computational domain when compared to the first order approach. This is especially true if a high accuracy is needed for the drag. Note that the additional computational time needed for the evaluation of the second order boundary terms is negligible. Therefore, the reduction of the diameter of the computational domain induced by the second order terms leads to direct and drastic benefits with regard to the overall computation time.

Due to the symmetry of the body leading to zero lift, all terms involving b in the proposed boundary conditions were inactive in the preceding test case. In order to check their relative role we consider a second body which consists of the NACA profile 64-015 shown in Figure 1. In order to obtain values of the lift which are comparable to the drag (so that b is comparable in size to d, see (36)), we consider this setup at a Reynolds number Re = 1000. The resulting values for drag and lift are given in Table 2. Similarly to the previous benchmark problem we also plot in Figure 6 the relative error of drag and lift as a function of domain size considering the different variants of boundary conditions as given in Table 1. The results show that the terms of the boundary conditions that include the lift effects only marginally influence the relative error of drag and lift at the level of the absolute error and range of Reynolds numbers computed here.

To summarize, the use of second order boundary conditions for exterior flows is not of academic value only but is very relevant in numerical simulations. When compared to the first order boundary conditions used in [6] their use allows a further important reduction of the computational domain, especially at low Reynolds numbers. Numerical evidence shows, however, that the boundary terms related to the effects of the lift which appear for non symmetric bodies do not contribute in an essential way to the accuracy of the solution when measured in terms of drag and lift.

Notation	Order	First order equations	b	Second order equations	b
sym	1	(37),(38)	$= 0$	-	-
nonsym	1	(37),(38)	$\neq 0$	-	-
sym/sym	2	(37),(38)	$= 0$	(39),(40),(41)	$= 0$
nonsym/sym	2	(37),(38)	$\neq 0$	(39),(40),(41)	$= 0$
nonsym/nonsym	2	(37),(38)	$\neq 0$	(39),(40),(41)	$\neq 0$

Table 1. Definition of the notation for the different variants of first and second order non homogeneous adaptive boundary conditions discussed in the paper.

Configuration	drag	lift
homogeneous Dirichlet	6.691	9.046
sym	6.626	8.925
nonsym	6.624	8.923
nonsym/sym	6.609	8.888
nonsym/nonsym	6.607	8.894

Table 2: Computed values of the drag and lift on a domain of diameter 10 for the configuration depicted in Figure 1 (Re = 1000). An approximation of the exact values as determined by a large scale computation are: drag ≈ 6.58 and lift ≈ 8.81.

5 Appendix I

In this appendix we give some more details concerning the construction of the asymptotic expansion. We start by explaining the procedure to first order. From (17) and (18) we have for ω_1,

$$\omega_1(x,y) = \frac{d}{x}\varphi''_{1,1}(\frac{y}{\sqrt{x}}) \ . \tag{53}$$

We have that $\int_0^\infty dx \int_{\mathbf{R}} dy \ \omega_1(x,y) = 0$, and therefore

$$b_1 = b + \frac{1}{2}\int_\Omega \omega_1(x,y) \ dxdy = b - \frac{1}{2}\int_{B_+} \omega_1(x,y) \ dxdy \ ,$$

where $\mathbf{B}_+ = \{(x,y) \in \mathbf{B} \,|\, x > 0\}$. Next, since

$$\int_\Omega G(x-x_0,y-y_0) \ \omega_1(x_0,y_0) \ dx_0 dy_0 = \int_0^\infty dx_0 \int_{\mathbf{R}} dy_0 \ G(x-x_0,y-y_0) \ \omega_1(x_0,y_0)$$
$$- \int_{B_+} G(x-x_0,y-y_0) \ \omega_1(x_0,y_0) \ dx_0 dy_0 \ ,$$

we have for ψ_1,

$$\psi_1(x,y) = 2b \ G(x,y) - \int_0^\infty dx_0 \int_{\mathbf{R}} dy_0 \ G(x-x_0,y-y_0) \ \omega_1(x_0,y_0)$$
$$- \int_{B_+} (G(x,y) - G(x-x_0,y-y_0)) \ \omega_1(x_0,y_0) \ dx_0 dy_0 \ . \tag{54}$$

The term in the second line in (54) is bounded by const./r and will be neglected. Using (53) and integrating twice by parts and using (33) leads to

$$\psi_1(x,y) \approx 2b\, G(x,y) - d\int_0^\infty dx_0 \int_{\mathbf{R}} dy_0\; G(x-x_0,y-y_0)\,\frac{1}{x_0}\varphi_{1,1}''\left(\frac{y_0}{\sqrt{x_0}}\right)$$

$$= 2b\, G(x,y) - d\int_0^\infty dx_0 \int_{\mathbf{R}} dy_0\; \partial_y G(x-x_0,y-y_0)\,\frac{1}{\sqrt{x_0}}\varphi_{1,1}'\left(\frac{y_0}{\sqrt{x_0}}\right)$$

$$= 2b\, G(x,y) - d\int_0^\infty dx_0 \left[\partial_y G(x-x_0,y-y_0)(\mathrm{erf}(\tfrac{1}{2}\frac{y_0}{\sqrt{x_0}})+1)\right]_{-\infty}^{0}$$

$$- d\int_0^\infty dx_0 \left[\partial_y G(x-x_0,y-y_0)(\mathrm{erf}(\tfrac{1}{2}\frac{y_0}{\sqrt{x_0}})-1)\right]_{0}^{\infty}$$

$$- d\int_0^\infty dx_0 \int_{\mathbf{R}} dy_0\; \partial_y^2 G(x-x_0,y-y_0)(\mathrm{erf}(\frac{y_0}{\sqrt{x_0}})-\mathrm{sign}(y_0))\;.$$

Since $\left(\partial_x^2 + \partial_y^2\right) G(x-x_0,y-y_0) = \delta(x-x_0)\delta(y-y_0)$, we therefore find that

$$\psi_1(x,y) \approx 2b\, G(x,y) - 2d\int_0^\infty \partial_y G(x-x_0,y)\, dx_0 - d\,\theta(x)(\mathrm{erf}(\frac{y}{\sqrt{x}})-\mathrm{sign}(y))$$

$$+ \partial_x^2\left(d\int_0^\infty dx_0 \int_{\mathbf{R}} dy_0\; G(x-x_0,y-y_0)(\mathrm{erf}(\frac{y_0}{\sqrt{x_0}})-\mathrm{sign}(y_0))\right)\;.$$

The last term is again bounded by const./r. We have that

$$\partial_y G(x-x_0,y) = \frac{1}{2\pi}\frac{y}{(x-x_0)^2+y^2}\;,$$

an therefore that

$$\int_0^\infty \partial_y G(x-x_0,y)\, dx_0 = -H(x,y)\;,$$

where

$$H(x,y) = \frac{1}{2\pi}\mathrm{Im}[\log(-x-iy)] = \frac{1}{2\pi}\arctan(\frac{y}{x}) - \frac{1}{2}\theta(x)\mathrm{sign}(y)\;.$$

Modulo terms bounded by const./r we therefore find the following local approximation $\psi_{1,\mathrm{loc}}$ of ψ_1

$$\psi_{1,\mathrm{loc}}(x,y) = 2b\, G(x,y) + 2d\, H(x,y) - d\,\theta(x)(\mathrm{erf}(\tfrac{1}{2}\frac{y}{\sqrt{x}})-\mathrm{sign}(y))\;,$$

from which (37) follows using (19) and (20), respectively.

Next we compute local approximations for the second and third order terms. Let $x_+ > 0$ be "to the right of $\mathbf{B}$", i.e., $x_+ > \sup_x\{x \in \mathbf{R}\,|\,(x,y) \in \mathbf{B}$ for some $y\}$ and let $\mathbf{B}_{+,\infty} = \{(x,y) \in \mathbf{R}^2\,|\,0 < x < x_+\}$. Using the definitions we have, for $i = 1,2$, that $\int_{x_+}^\infty dx \int_{\mathbf{R}} dy\; \omega_i(x,y) = 0$, and therefore that $b_i = b_{i-1} + \frac{1}{2}\int_{\mathbf{B}_{+,\infty}} \omega_i(x,y)\, dxdy$. Therefore,

$$\psi_i(x,y) = \psi_{i-1}(x,y) + \int_\Omega (G(x,y) - G(x-x_0,y-y_0))\,\omega_i(x_0,y_0)\, dx_0 dy_0$$

$$= \psi_{i-1}(x,y) - \int_{x_+}^\infty dx_0 \int_{\mathbf{R}} dy_0 G(x-x_0,y-y_0)\omega_i(x_0,y_0)\, dx_0 dy_0$$

$$+ \int_{\mathbf{B}_{+,\infty}} (G(x,y) - G(x-x_0,y-y_0))\,\omega_i(x_0,y_0)\, dx_0 dy_0\;. \tag{55}$$

The last term in (55) is bounded by const./r and will be neglected. For the contribution of $\varphi_{2,1}$ to ψ_2

we have

$$-\int_{x_+}^{\infty} dx_0 \int_{\mathbf{R}} dy_0 \ G(x-x_0, y-y_0) \ \frac{\log(x_0)}{x_0^{3/2}} \varphi_{2,1}''(\frac{y_0}{\sqrt{x_0}})$$

$$= -\int_{x_+}^{\infty} dx_0 \int_{\mathbf{R}} dy_0 \ \partial_y G(x-x_0, y-y_0) \ \frac{\log(x_0)}{x_0} \varphi_{2,1}'(\frac{y_0}{\sqrt{x_0}})$$

$$= -\int_{x_+}^{\infty} dx_0 \int_{\mathbf{R}} dy_0 \ \partial_y^2 G(x-x_0, y-y_0) \frac{\log(x_0)}{\sqrt{x_0}} \frac{bd}{\pi^{3/2}} e^{-\frac{y_0^2}{4x_0}}$$

$$= -\theta(x-x_+)\frac{\log(x)}{\sqrt{x}} \frac{bd}{\pi^{3/2}} e^{-\frac{y^2}{4x}}$$

$$+ \partial_x^2 \left(\int_{x_+}^{\infty} dx_0 \int_{\mathbf{R}} dy_0 \ G(x-x_0, y-y_0)\frac{\log(x_0)}{\sqrt{x_0}} \frac{bd}{\pi^{3/2}} e^{-\frac{y_0^2}{4x_0}} \right)$$

$$\approx -\theta(x)\frac{\log(x)}{\sqrt{x}} \frac{bd}{\pi^{3/2}} e^{-\frac{y^2}{4x}} \ , \tag{56}$$

where the last approximation sign means that we have again neglected terms bounded by const./r. Similarly we find for the contribution of $\varphi_{3,1}$ to ψ_3,

$$-\int_{x_+}^{\infty} dx_0 \int_{\mathbf{R}} dy_0 \ G(x-x_0, y-y_0) \ \frac{\log(x_0)^2}{x_0^2} \varphi_{3,1}''(\frac{y_0}{\sqrt{x_0}})$$

$$\approx \theta(x)\frac{\log(x)^2}{x} \frac{b^2 d}{4\pi^{5/2}} \frac{y}{\sqrt{x}} e^{-\frac{y^2}{4x}} \ . \tag{57}$$

We finally discuss the contribution of $\varphi_{2,2}$ to ψ_2. We have (we only treat the case $c_{2,2} = 0$)

$$-\int_{x_+}^{\infty} dx_0 \int_{\mathbf{R}} dy_0 \ G(x-x_0, y-y_0) \ \frac{1}{x_0^{3/2}} \varphi_{2,2}''(\frac{y_0}{\sqrt{x_0}})$$

$$= -\int_{x_+}^{\infty} dx_0 \int_{\mathbf{R}} dy_0 \ \partial_y G(x-x_0, y-y_0) \ \frac{1}{x_0} \varphi_{2,2}'(\frac{y_0}{\sqrt{x_0}})$$

$$= d^2 \int_{x_+}^{\infty} dx_0 \left[\partial_y G(x-x_0, y-y_0)\frac{1}{\sqrt{x_0}}(f(\frac{y_0}{\sqrt{x_0}}) + f_\infty) \right]_{-\infty}^{0}$$

$$+ d^2 \int_{x_+}^{\infty} dx_0 \left[\partial_y G(x-x_0, y-y_0)\frac{1}{\sqrt{x_0}}(f(\frac{y_0}{\sqrt{x_0}}) - f_\infty) \right]_{0}^{\infty}$$

$$+ d^2 \int_{x_+}^{\infty} dx_0 \int_{\mathbf{R}} dy_0 \ \partial_y^2 G(x-x_0, y-y_0)\frac{1}{\sqrt{x_0}}(f(\frac{y_0}{\sqrt{x_0}}) - f_\infty \mathrm{sign}(y_0))$$

$$= 2d^2 f_\infty \int_{0}^{\infty} \frac{dx_0}{\sqrt{x_0}} \partial_y G(x-x_0, y) + \theta(x)\frac{d^2}{\sqrt{x}}(f(\frac{y}{\sqrt{x}}) - f_\infty \mathrm{sign}(y))$$

$$+ 2d^2 f_\infty \int_{0}^{x_+} \frac{dx_0}{\sqrt{x_0}} \partial_y G(x-x_0, y) +$$

$$- \partial_x^2 \left(d^2 \int_{x_+}^{\infty} dx_0 \int_{\mathbf{R}} dy_0 \ G(x-x_0, y-y_0)\frac{1}{\sqrt{x_0}}(f(\frac{y_0}{\sqrt{x_0}}) - f_\infty \mathrm{sign}(y_0)) \right) \ . \tag{58}$$

The last two terms are again bounded by const./r, and we might be tempted to neglect them as in the previous cases. In contrast to all the other terms considered so far the remaining local approximation is however not sufficiently differentiable in y at $y = 0$ and $x > 0$. Namely,

$$\int_{0}^{\infty} \frac{dx_0}{\sqrt{x_0}} \partial_y G(x-x_0, y) \ dx_0 = \frac{1}{2} H_2(x, y) \ ,$$

where

$$H_2(x, y) = \mathrm{Im}[\frac{1}{\sqrt{-x-iy}}] = \frac{1}{2}\mathrm{sign}(y)\frac{r_2}{r} \ ,$$

13

with $r = \sqrt{x^2 + y^2}$ and $r_2 = \sqrt{2r + 2x}$. For $x > 0$ fix and y small we have,

$$H_2(x, y) = \frac{\mathrm{sign}(y)}{\sqrt{x}}(1 - \frac{3}{8}(\frac{y}{x})^2 + \mathcal{O}((\frac{y}{x})^4)) , \tag{59}$$

and it is now easy to see using (19) and (20) that the contribution of H_2 to the local approximation of u_2 and v_2 is not twice differentiable. We are therefore forced to extract in (58) an additional term that compensates the contribution proportional to $\mathrm{sign}(y)y^2$ in (59), and we finally get from (56)-(58) the following local approximations $\psi_{2,\mathrm{loc}}$ and $\psi_{3,\mathrm{loc}}$ of ψ_2 and ψ_3,

$$\psi_{2,\mathrm{loc}}(x, y) = \psi_{1,\mathrm{loc}}(x, y) - \theta(x)\frac{\log(x)}{\sqrt{x}} \frac{bd}{\pi^{3/2}} e^{-\frac{y^2}{4x}}$$

$$+ d^2 f_\infty H_2(x, y) + \theta(x) \frac{d^2}{x} (f(x, y) - f_\infty \mathrm{sign}(y))$$

$$+ \lambda\, \theta(x)\, d^2 f_\infty \frac{3}{8} \frac{1}{x^{3/2}} \frac{y}{\sqrt{x}}(1 + \frac{|y|}{\sqrt{x}}) e^{-\frac{y^2}{4x}}$$

$$\psi_{3,\mathrm{loc}}(x, y) = \psi_{2,\mathrm{loc}}(x, y) + \theta(x)\frac{\log(x)^2}{x} \frac{b^2 d}{4\pi^{5/2}} \frac{y}{\sqrt{x}} e^{-\frac{y^2}{4x}} ,$$

from which (39)-(42) follow using (19) and (20), respectively.

We still have to check that with the above choices for $\varphi_{i,j}$ the equation (14) is satisfied asymptotically as claimed in (32). To first order one can show (using the computer-algebra system Maple for example) that

$$\lim_{x \to \infty} x^2\, W(1 + u_1, v_1, \omega_1)(x, \sqrt{x}z) = 0 ,$$

because $L_1(\varphi_{1,1})(z) = 0$, where for $n \in \mathbf{N}$,

$$L_n(f)(z) = f''''(z) + \frac{1}{2}zf'''(z) + \frac{1+n}{2}f''(z) .$$

The function $\varphi_{1,1}$ is the (up to a constant) unique solution of $L_1(f) = 0$ with derivatives decaying faster than exponential at infinity. At order N of the expansion the operator L_N has to be discussed. The second order operator L_2 contains in its kernel the function $z \mapsto e^{-z^2/4}$, and for this reason the equation $L_2(f) = g$ with g a smooth function of rapid decrease, say, has typically a solution f whose even part decays only algebraically at infinity (see [22], [40]). This is not acceptable in our case since the vorticity is supposed to decay faster than exponential transversal to the wake. This means that the correct asymptotic expansion has a logarithmic second order term $\varphi_{2,1}$ (see [40] for a description of the ideas). This additional term permits to adjust the inhomogeneity g in the equation for $\varphi_{2,2}$ such that the solution is of rapid decrease. It turns out that in our case the logarithmic correction term $\varphi_{2,1}$ can be chosen such that the equation for $\varphi_{2,2}$ has no even inhomogeneous term. More precisely we have

$$\lim_{x \to \infty} x^{5/2}\, W(1 + u_1 + u_2, v_1 + v_2, \omega_1 + \omega_2)(x, \sqrt{x}z) = 0 , \tag{60}$$

because $L_2(\varphi_{2,1})(z) = 0$ and $L_2(\varphi_{2,2})(z) = -ze^{-z^2/2}/(2\pi)$ (this is the derivative of equation (34)). Finally, to third order we have to discuss L_3. This time the problem is that L_3 contains in its kernel the function $z \mapsto ze^{-z^2/4}$, and for this reason the equation $L_3(f) = g$ has typically a solution f whose odd part decays only algebraically at infinity. In our case, because of the logarithmic second order term, this problem already arises at the level of the equation for $\varphi_{3,2}$. The correct asymptotic expansion therefore contains a quadratic logarithmic third order term $\varphi_{3,1}$. This additional term permits to adjust the inhomogeneity g in the equation for $\varphi_{3,2}$ such that the solution is of rapid decrease. It turns out that in our case the logarithmic correction term $\varphi_{3,1}$ can be chosen such that the equation for $\varphi_{3,2}$ has no odd inhomogeneous term. Finally, $\varphi_{3,2}$ has to be chosen such that $\varphi_{3,3}$ is of rapid decrease. More precisely, we have

$$\lim_{x \to \infty} \frac{x^3}{\log(x)}\, W(1 + u_1 + u_2 + u_3, v_1 + v_2 + v_3, \omega_1 + \omega_2 + \omega_3)(x, \sqrt{x}z) = 0 , \tag{61}$$

because $L_3(\varphi_{3,1})(z) = 0$ and $L_3(\varphi_{3,2})(z) = \left(e^{-\frac{1}{2}z^2}/(2\pi^2)\right)''$. Explicitly we find,

$$\varphi_{3,2}(z) = -\frac{d^2}{2\pi^{3/2}}(1 - \frac{d}{4\sqrt{3}})\, ze^{-\frac{z^2}{4}} - c_{2,2}b^2 \frac{z}{2\pi}\, e^{-\frac{z^2}{4}} + f_{3,2}(z) ,$$

with $f_{3,2}$ satisfying $f_{3,2}(0) = -1/(2\pi^2)$, $f'_{3,2}(0) = f''_{3,2}(0) = f'''_{3,2}(0) = 0$. Note that $f_{3,2}$ is an even function decaying faster than exponential at infinity. See Figure 3 for a graph of the function $f_{3,2}$.

6 Appendix II

In this appendix we recall the computation of drag and lift through surface integrals. We also recall the relation between the lift and the average vorticity, *i.e.*, the fact that b is given by (31). Let $\mathbf{u}$, p be a solution of the Navier-Stokes equations (9), (10) subject to the boundary conditions (11), (12), and let $\mathbf{e}$ be some arbitrary unit vector in $\mathbf{R}^2$. Multiplying (9) with $\mathbf{e}$ leads to

$$- (\mathbf{u} \cdot \nabla)(\mathbf{u} \cdot \mathbf{e}) + \Delta (\mathbf{u} \cdot \mathbf{e}) - \nabla \cdot (p\mathbf{e}) = 0 . \tag{62}$$

Since

$$\nabla \cdot ((\mathbf{u} \cdot \mathbf{e}) \mathbf{u}) = \mathbf{u} \cdot (\nabla (\mathbf{u} \cdot \mathbf{e})) + (\mathbf{u} \cdot \mathbf{e})(\nabla \cdot \mathbf{u}) = (\mathbf{u} \cdot \nabla)(\mathbf{u} \cdot \mathbf{e}) ,$$
$$\Delta (\mathbf{u} \cdot \mathbf{e}) = \nabla \cdot ([\nabla \mathbf{u} + (\nabla \mathbf{u})^T] \cdot \mathbf{e}) ,$$

equation (62) can be written as $\nabla \cdot \mathbf{P}(\mathbf{e}) = 0$, where

$$\mathbf{P}(\mathbf{e}) = -(\mathbf{u} \cdot \mathbf{e}) \mathbf{u} + [\nabla \mathbf{u} + (\nabla \mathbf{u})^T] \cdot \mathbf{e} - p\mathbf{e} , \tag{63}$$

i.e., the vector field $\mathbf{P}(\mathbf{e})$ is divergence free. Therefore, applying Gauss's theorem to the region Ω_S (see Figure 2) we find that

$$\int_{\partial\Omega} \mathbf{P}(\mathbf{e}) \cdot \mathbf{n} \, d\sigma = \int_S \mathbf{P}(\mathbf{e}) \cdot \mathbf{n} \, d\sigma , \tag{64}$$

with the choice of normal vectors as indicated in Figure 2. We have that $\mathbf{P}(\tilde{\mathbf{e}}) \cdot \mathbf{e} = \mathbf{P}(\mathbf{e}) \cdot \tilde{\mathbf{e}}$ for any two unit vectors $\mathbf{e}$ and $\tilde{\mathbf{e}}$, and therefore, since $\mathbf{e}$ is arbitrary, it follows from (64) that

$$\int_{\partial\Omega} \mathbf{P}(\mathbf{n}) \, d\sigma = \int_S \mathbf{P}(\mathbf{n}) \, d\sigma . \tag{65}$$

Since $\mathbf{u} = 0$ on $\partial\Omega$, we finally get from (65) and (63) that the total force the fluid exerts on the body is

$$\mathbf{F} = \int_{\partial\Omega} \Sigma(\mathbf{u}, p)\mathbf{n} \, d\sigma = \int_S \left(-(\mathbf{u} \cdot \mathbf{n}) \mathbf{u} + [\nabla \mathbf{u} + (\nabla \mathbf{u})^T]\mathbf{n} - p\mathbf{n} \right) \, d\sigma ,$$

with $\Sigma(\mathbf{u}, p) = \nabla \mathbf{u} + (\nabla \mathbf{u})^T - p$ the Stress tensor. In dimension-full variables we have

$$\tilde{\mathbf{F}} = \int_{\tilde{S}} \left(-\rho (\tilde{\mathbf{u}} \cdot \mathbf{n}) \tilde{\mathbf{u}} + \mu[\tilde{\nabla}\tilde{\mathbf{u}} + (\tilde{\nabla}\tilde{\mathbf{u}})^T]\mathbf{n} - \tilde{p}\mathbf{n} \right) \, d\tilde{\sigma} = \rho u_\infty^2 \ell \, \mathbf{F} . \tag{66}$$

The force $\mathbf{F}$ is traditionally decomposed into a component F parallel to the flow at infinity called drag and a component L perpendicular to the flow at infinity called lift. Note that $\mathbf{F}$ is independent of the choice of S. This has the important consequence that F and L can be computed from the dominant terms $\mathbf{u}_1$ and p_1 of the velocity field and the pressure. Also, since $\lim_{|y|\to\infty} \mathbf{u}(x, y) = (1, 0)$ and $\lim_{|y|\to\infty} p(x, y) = 0$, we can replace S by two vertical lines, one at $-x < 0$ to the left of the body and one at $x > 0$ to the right of the body. Therefore we have, modulo terms that vanish as x goes to infinity,

$$F = \lim_{x\to\infty} \int_{\mathbf{R}} \left(-(1 - \frac{d}{\sqrt{\pi}} \frac{1}{\sqrt{x}} e^{-\frac{y^2}{4x}} + u_{1,1,E}(x,y))^2 + (1 + u_{1,1,E}(-x,y))^2 \right) \, dy$$
$$+ \frac{1}{2} \lim_{x\to\infty} \int_{\mathbf{R}} \left((1 + u_{1,1,E}(x,y))^2 - 1 + v_{1,1,E}(x,y)^2 \right) \, dy$$
$$- \frac{1}{2} \lim_{x\to\infty} \int_{\mathbf{R}} \left((1 + u_{1,1,E}(-x,y))^2 - 1 + v_{1,1,E}(-x,y)^2 \right) \, dy$$
$$= \int_{\mathbf{R}} \left(\frac{2d}{\sqrt{\pi}} \frac{1}{\sqrt{x}} e^{-\frac{y^2}{4x}} - 4\frac{d}{\pi} \frac{x}{x^2+y^2} \right) \, dy + \frac{1}{2} \int_{\mathbf{R}} \left(4\frac{d}{\pi} \frac{x}{x^2+y^2} \right) \, dy = 2d \tag{67}$$

and

$$L = -\lim_{x \to \infty} \int_{\mathbf{R}} \left(1 - \frac{d}{\sqrt{\pi}} \frac{1}{\sqrt{x}} e^{-\frac{y^2}{4x}} + u_{1,1,E}(x,y) \right) \left(-\frac{d}{2\sqrt{\pi}} \frac{y}{x^{3/2}} e^{-\frac{y^2}{4x}} + v_{1,1,E}(x,y) \right) \, dy$$
$$+ \lim_{x \to \infty} \int_{\mathbf{R}} (1 + u_{1,1,E}(-x,y)) v_{1,1,E}(-x,y) \, dy$$
$$= -\int_{\mathbf{R}} \left(-\frac{b}{\pi} \frac{x}{x^2 + y^2} \right) \, dy + \int_{\mathbf{R}} \left(-\frac{b}{\pi} \frac{-x}{x^2 + y^2} \right) \, dy = 2b \, , \tag{68}$$

and equation (36) now follows using (66). Finally, in order to show identity (31), we use Stokes' theorem which relates the average vorticity to a line integral along $\partial \mathbf{B}$ and a line integral along S in the limit when S goes to infinity. The integral along $\partial \mathbf{B}$ is zero since $\mathbf{u}|_{\partial \mathbf{B}} = 0$ and the limit of the integral along S can be computed as above by first taking the limit where S is replaced by two vertical lines and then the limit when x goes to infinity.

References

[1] C. J. Amick, *On the asymptotic form of Navier-Stokes flow past a body in the plane*, Journal of differential equations **91** (1991), 149–167.

[2] M. B. Baker, *Cloud microphysics and climate*, Science **276** (1997), 279–306.

[3] W. Bao, *Artificial boundary conditions for incompressible Navier-Stokes equations: A well-posed result*, Comput. Meth. Appl. Mech. Engr. **188** (2000), 595–611.

[4] G. K. Batchelor, *A introduction to fluid dynamics*, Cambridge University Press, 1967.

[5] S. Berger, *Laminar wakes*, American Elsevier Publishing Company, Inc., 1971.

[6] S. Bönisch, V. Heuveline, and P. Wittwer, *Adaptive boundary conditions for exterior flow problems*, Journal of Mathematical Fluid Mechanics, to appear (2003).

[7] S.C. Brenner and R.L. Scott, *The mathematical theory of finite element methods*, Springer, Berlin-Heidelberg-New York, 1994.

[8] F. Brezzi and R. Falk, *Stability of higher-order Hood-Taylor methods*, SIAM J. Numer. Anal. **28** (1991), no. 3, 581–590.

[9] B. H. Carmichael, *Low Reynolds number airfoil survey*, NASA CR-1165803 (1981).

[10] A. Chorin and J. E. Marsden, *A mathematical introduction to fluid mechanics*, Interscience Publishers, Ltd., London, 1992.

[11] R. Eppler and D. M. Somers, *Low speed airfoil design and analysis*, Advanced Technology Airfoil Research, Volume I (1979).

[12] _____, *A computer program for the design and analysis of low-speed airfoils*, NASA TM-80210 (1981).

[13] G. P. Galdi, *An introduction to the mathematical theory of the Navier-Stokes equations: Linearized steady problems*, Springer Tracts in Natural Philosophy, Vol. 38, Springer-Verlag, 1998.

[14] _____, *An introduction to the mathematical theory of the Navier-Stokes equations: Nonlinear steady problems*, Springer Tracts in Natural Philosophy, Vol. 39, Springer-Verlag, 1998.

[15] G.P. Galdi, *An introduction to the mathematical theory of the Navier-Stokes equations: Linearized steady problems*, Springer Tracts in Natural Philosophy, Vol. 38, Springer-Verlag, 1998.

[16] _____, *An introduction to the mathematical theory of the Navier-Stokes equations: Nonlinear steady problems*, Springer Tracts in Natural Philosophy, Vol. 39, Springer-Verlag, 1998.

[17] _____, *On the existence of symmetric steady-state solutions to the plane exterior Navier-Stokes problem for a large Reynolds number*, Advances in Fluid Dynamics, Quaderni Di Matematica della II Universita' di Napoli **4** (1999), 1–25.

[18] T. Gallay, *A center-stable manifold theorem for differential equations in Banach spaces*, Commun. Math. Phys. **152** (1993), 249–268.

[19] Th. Gallay and C.E. Wayne, *Invariant manifolds and the long-time asymptotics of the navier-stokes and vorticity equations on r^2*, Arch. Rat. Mech. Anal. **163** (2002), 209–258.

[20] _____, *Long-time asymptotics of the navier-stokes and vorticity equations on r^3*, Phil. Trans. Roy. Soc. Lond. **360** (2002), 2155–2188.

[21] M. Giles, M. Larson, M. Levenstam, and E. Süli, *Adaptive error control for finite element approximations of the lift and drag coefficients in viscous flow*, Tech. Report NA-97/06, Oxford University Computing Laboratory, 1997.

[22] S. Goldstein, *Lectures on fluid mechanics*, Interscience Publishers, Ltd., London, 1957.

[23] F. Haldi and P. Wittwer, *Leading order down-stream asymptotics of non-symmetric stationary Navier-Stokes flows in two dimensions*, Journal of Mathematical Fluid Mechanics, to appear (2003).

[24] L. Halpern, *Spectral methods in polar coordinates for the Stokes problem. application to computation in unbounded domains.*, Mathematics of Computation **65** (1996), 507–531.

[25] V. Heuveline, **HiFlow** *a general finite element C++ package for 2D/3D flow simulation*, www.hiflow.de (2000).

[26] _____, *On higher-order mixed FEM for low Mach number flows: Application to a natural convection benchmark problem*, Int. J. Numer. Math. Fluids **41** (2003), no. 12, 1339–1356.

[27] J. G. Heywood, R. Rannacher, and S. Turek, *Artificial boundaries and flux and pressure conditions for the incompressible navier-stokes equations*, Int. J. Numer. Math. Fluids **22** (1992), 325–352.

[28] P. Hood and C. Taylor, *A numerical solution of the navier-stokes equations using the finite element techniques*, Comp. and Fluids **1** (1973), 73–100.

[29] C.T. Kelley, *Iterative methods for linear and nonlinear equations*, Frontiers in Applied Mathematics, vol. 16, SIAM, Philadelphia, 1995.

[30] C. L. Ladson, C. W. Brooks, A. S. Hill Jr., and D. W. Sproles, *Computer program to obtain ordinates for NACA airfoils*, NASA Technical Memorandum 4741 (1996).

[31] L. Landau and E. Lifchitz, *Physique théorique, tome 6, mécanique des fluides*, Editions MIR, 1989.

[32] T. J. Mueller, *Fixed and flapping wing aerodynamics for micro air vehicle applications*, vol. 195, AIAA, 2001.

[33] S. A. Nazarov and M. Specovius-Neugebauer, *Nonlinear artificial boundary conditions with pointwise error estimates for the exterior three dimensional Navier-Stokes problem*, Math. Nachr., to appear (2003).

[34] R. Rannacher, *Finite element methods for the incompressible Navier-Stokes equations*, Fundamental Directions in Mathematical Fluid Mechanics (Galdi Giovanni et al., ed.), Advances in Mathematical Fluid Mechanics, Birkhäuser, 2000.

[35] Y. Saad, *Iterative methods for sparse linear systems*, Computer Science/Numerical Methods, PWS Publishing Company, 1996.

[36] H. Schlichting and K. Gersten, *Boundary layer theory*, Springer, 1999.

[37] I. J. Sobey, *Introduction to interactive boundary layer theory*, Oxford University Press, 2000.

[38] K. Stewartson, *On asymptotic expansions in the theory of boundary layers*, J. Maths Physics **36** (1957), 173–191.

[39] S. Turek, *Efficient solvers for incompressible flow problems. an algorithmic and computational approach*, Lecture notes in Computational Science and Engineering, Springer, 1999.

[40] M. van Dyke, *Perturbation methods in fluid mechanics*, The parabolic press, Stanford, California, 1975.

[41] S. Vanka, *Block-implicit multigrid calculation of two-dimensional recirculating flows*, Comp. Meth. Appl. Mech. Eng. **59** (1986), no. 1, 29–48.

[42] P. K. Wang and W. Ji, *Collision efficiencies of ice crystals at low-intermediate Reynolds numbers colliding with supercooled cloud droplets: a numerical study*, Journal of the atmospheric sciences **57** (2000), 1001–1009.

[43] E. Wayne, *Invariant manifolds for parabolic partial differential equations on unbounded domains*, Arch. Rational Mech. Anal. **138** (1997), 279–306.

[44] H. Werle, *Le tunnel hydrodynamique au service de la recherche aérospatiale, publication no 156*, ONERA, Oficce National d'études et de recherches aérospaciales, 1974.

[45] P. Wesseling, *An introduction to multigrid methods*, Wiley, Chichester, 1992.

[46] P. Wesseling and C.W. Oosterlee, *Geometric multigrid with applications to computational fluid dynamics*, J. Comp. Appl. Math. **128** (2001), 311–334.

[47] P. Wittwer, *On the structure of Stationary Solutions of the Navier-Stokes equations*, Commun. Math. Phys. **226** (2002), 455–474.

[48] _____, *Leading order down-stream asymptotics of non-symmetric stationary Navier-Stokes flows in three dimensions*, Geneva preprint (2003).

[49] _____, *Supplement: On the structure of stationary solutions of the Navier-Stokes equations*, Commun. Math. Phys. **234** (2003).
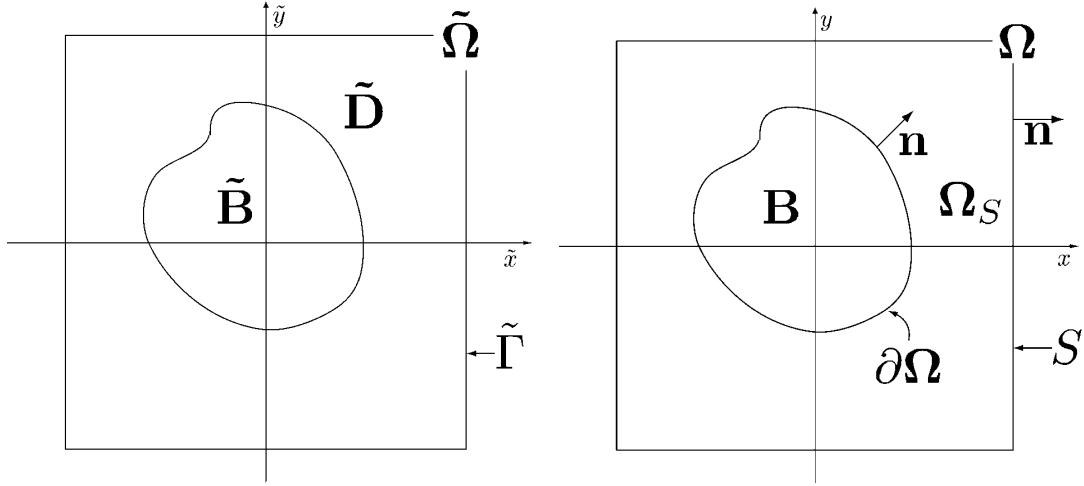
Figure 2. The body $\tilde{\mathbf{B}}$, the exterior domain $\tilde{\Omega}$, the computational domain $\tilde{\mathbf{D}}$ and the artificial boundary $\tilde{\Gamma}$ (left) and the surface S used in the the theorems of Gauss and Stokes and the definition of normal vectors on $\partial\Omega$ and S (right).
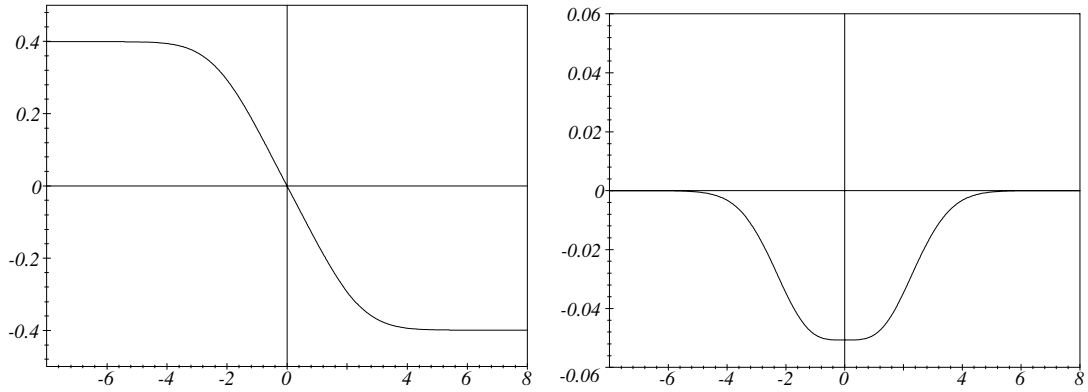

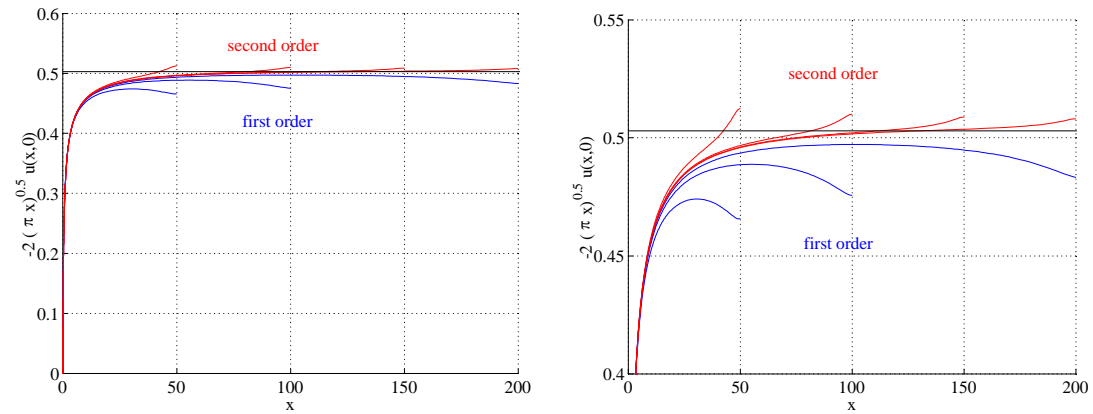Figure 3. The graph of the function f (left) and $f_{3,2}$ (right).

Figure 4. The scaled centerline velocity to first and second order (left) and zoom on the same quantities (right).
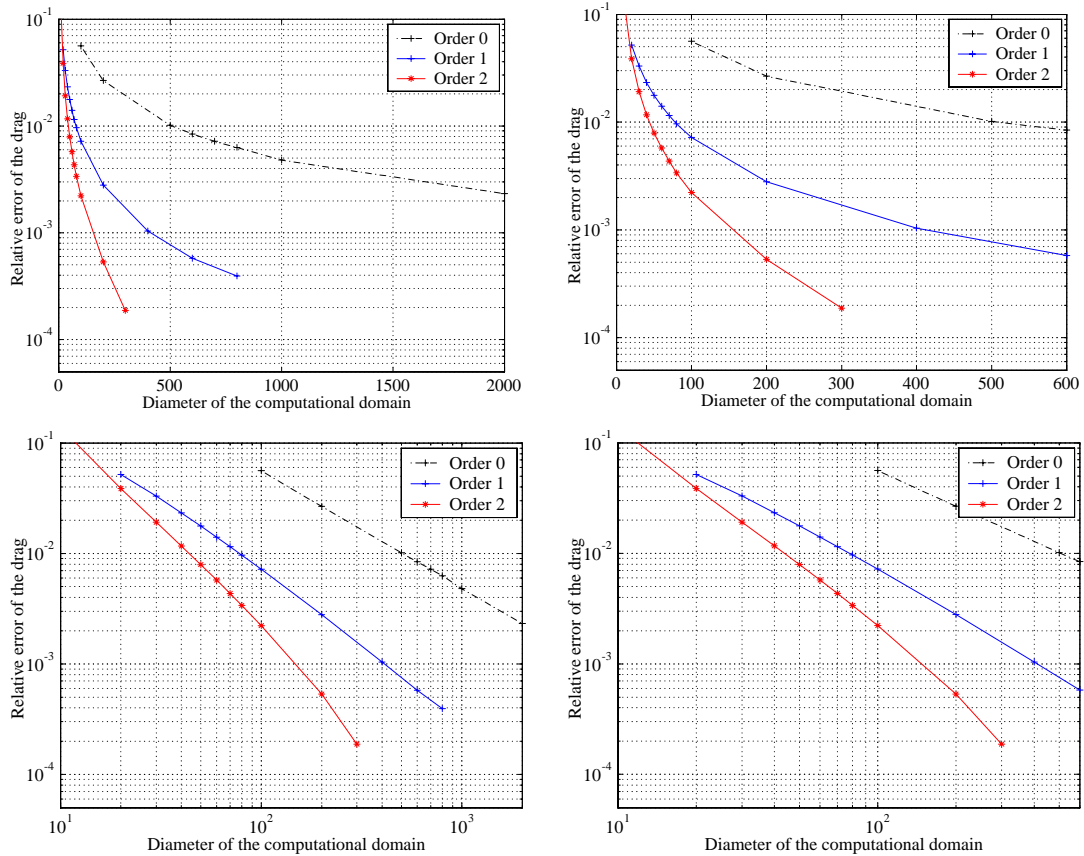
Figure 5. Plot of the relative error of the drag as a function of the domain diameter considering homogeneous Dirichlet boundary conditions and the adaptive boundary conditions to first and second order. From left to right and top to bottom the quantities are plotted in semilog plots un-zoomed and zoomed and in log/log plots un-zoomed and zoomed.
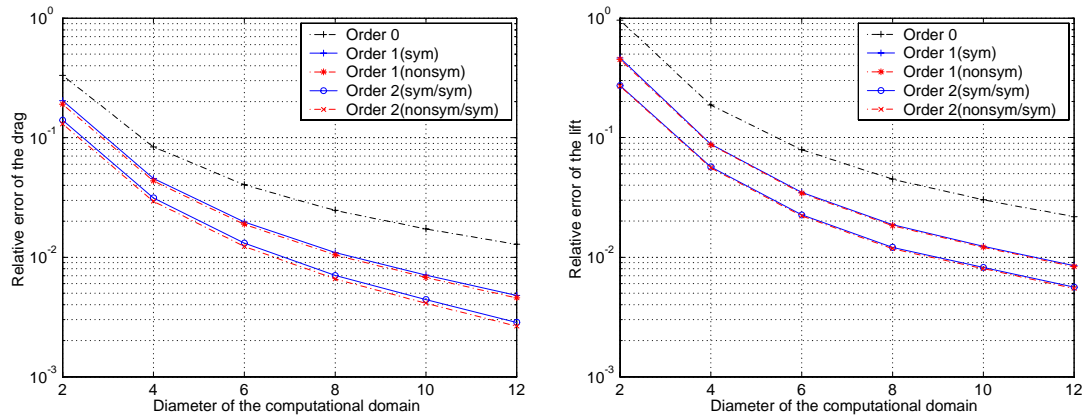

Figure 6. Plot of the relative error of the drag (left) and the lift (right) as a function of the domain diameter considering homogeneous Dirichlet boundary conditions and the adaptive boundary conditions to first and second order.